RSC Advances

PAPER

View Article Online
View Journal | View Issue

Cite this: *RSC Adv.*, 2021, **11**, 10075

Determination of cesium ions in environmental water samples with a magnetic multi-walled carbon nanotube imprinted potentiometric sensor†

Zhiming Wang, Long Wang, Cuo Zhou and Chunyan Sun*

Received 13th November 2020
Accepted 1st March 2021

DOI: 10.1039/d0ra09659h

rsc.li/rsc-advances

A potentiometric sensor, based on the glassy carbon electrode (GCE) modified with a magnetic multi-walled carbon nanotubes/cesium ion-imprinted polymer composite (MMWCNTs@Cs-IIP), is introduced for the detection of cesium(I). The IIP was synthesized using cesium ions as the template ions, chitosan as the functional monomer and glutaraldehyde as the cross-linking agent. The membrane, which was coated on the surface of the GCE, was prepared using MMWCNTs@Cs(I)-IIP as the modifier, PVC as the neutral carrier, 2-nitrophenyloctyl ether as the plasticizer and sodium tetraphenylborate as the lipophilic salt. The proposed sensor exhibited a Nernstian slope of 0.05954 V dec^{-1} in a working concentration range of 1×10^{-7} to 1×10^{-4} M (mol L^{-1}) with a detection limit of 4×10^{-8} M. The sensor exhibited high selectivity for cesium ions and was successfully applied for the determination of Cs(I) in real samples.

Introduction

Recently, the demand for cesium in the international market has increased significantly because cesium plays an increasingly important role in the national defense, aerospace, energy, materials, electronics and medicine fields.[1–3] Salt lake brine stores a considerable amount of cesium resources, but the composition of the brine system is complex. During the utilization process, the separation of cesium from co-existing elements such as magnesium, calcium, sodium and potassium is very important.[4–6] On the other hand, Cs is a very dangerous radioactive source. When accidentally released into the ground and sea, it must be immediately captured for public safety.[7,8] However, these issues have been rather challenging because the concentration of the Cs ions is usually much lower than those of the co-existing competing cations.[9]

Several instrumental methods including flame atomic absorption spectrometry (FAAS), inductively coupled plasma mass spectrometry (ICP-MS) and ion chromatography (IC) have been introduced for measuring cesium.[10–14] These techniques require expensive instruments and time-consuming sample pretreatments. Recently, much attention has been given to electrochemical methods due to their simplicity and low cost, but some problems involving the lack of sensitivity and selectivity have not been resolved.[15–17]

Ion imprinted technology is a versatile approach for the preparation of synthetic materials that are capable of recognizing template ions. The high selectivity of ion imprinting polymers (IIPs) arises from active recognition sites that are complementary to the shape and size of the imprinted ions.[18–20] Several IIPs-based potentiometric sensors have been reported for sensing ions.[21–24] However, most of the sensors are proposed for heavy metals detection, and cesium potentiometric sensors have rarely been reported.

Multiwalled carbon nanotubes (MWCNTs) and Fe_3O_4 nanoparticles (NPs) have also been employed in sensors as modification materials due to their large surface area, good stability, conductivity and electron transfer, which can improve the analytical sensitivity of the electrochemical sensor.[25–29] The integration of MWCNTs and Fe_3O_4 NPs is expected to provide a synergistic effect in electrochemical sensor construction.

In the present study, a Cs(I)-imprinted polymer-based magnetic multiwalled carbon nanotube (MMWCNTs@Cs(I)-IIP) was synthesized for the selective detection of cesium ions in aqueous solutions. The polymer could be easily separated with an external magnetic field without either additional centrifugation or filtration procedures. The MMWCNTs@Cs(I)-IIP was then used as an ionophore to prepare a PVC-based membrane covered on the surface of a glassy carbon electrode. Multi-walled carbon nanotubes are used as the substrate of cesium ion imprinted polymer, which has the advantages of high mechanical strength, stability under acidic conditions, non-swelling, large surface area, unique chemical properties and easy processing. Compared with previous work, the use of multi-walled carbon nanotubes as the base material improves the sensitivity and accuracy of ion-selective electrodes.[30] The performance of the prepared electrochemical sensor was investigated in detail by differential pulse voltammetry (DPV), cyclic voltammetry (CV) and chronopotentiometry. The developed sensor was effectively used for sensing of the Cs(I) ion in the collected environmental samples.

College of Chemical Engineering, Qinghai University, Xining 810016, China. E-mail: sunchunyan@qhu.edu.cn

† Electronic supplementary information (ESI) available. See DOI: 10.1039/d0ra09659h

Experimental

Chemicals and materials

MWCNTs (5–10 nm diameter, 5–15 μm length), CsCl, $FeCl_3 \cdot 6H_2O$ (AR), carboxylated chitosan (CTS, BR, water-soluble), ammonium persulfate (AR), sodium bisulfate (AR), aqueous acetic acid (AR), glutaraldehyde solution (50%), Nafion solution and tetrahydrofuran (THF, AR) were obtained from Aladdin Reagent Co., Ltd. (Shanghai, China). In addition, *o*-nitrophenyloctylether (*o*-NPOE), dibutylphthalate (DBP), sodium tetraphenylborate (NaTPB), high molecular weight polyvinylchloride (PVC) and sorbitol oleate (Span-80) were purchased from Macklin (Shanghai, China). The bare glassy carbon electrodes (GCEs) were purchased from Gaoss Union.

River water was collected from the Beichuan river in Xining. Industrial wastewater was collected from an aluminum factory in Xining. The sample of brine was collected from a salt lake in Qaidam Basin, Qinghai. All the real samples were filtered through a 0.45 μm polycarbonate membrane, and the pH value is adjusted to 6.5 with 0.1 mol L^{-1} HNO_3.

Apparatus

All the electrochemical measurements were obtained with a three-electrode system using a PGSTAT204 electrochemical workstation (Switzerland). The concentration of metal ions in the solution was determined using a flame atomic absorption spectrometer (FAAS, TAS990, Universal, China) or an inductively coupled plasma mass spectrometer (ICP-MS, Thermo, USA). Fourier transform infrared spectra in KBr were recorded in the range of 400–4000 cm^{-1} using a FT-IR BXII spectrometer (Perkin-Elmer, USA). Energy dispersive spectrometry (EDS) (JSM-5610LV/INCA, United Oxford Instruments) operated at 20 kV was performed to confirm the existence of elements in the Cs(I)-IIP. Scanning Electron Microscope (SEM) images were taken using a JEOL-SEM (JSM-7001F, USA) operated at 15 kV. Transmission Electron Microscopy (TEM) images were taken using a Tecnai TF20 G2 FEG-TEM at 200 kV accelerating voltage with a standard single tilt holder. Ultra-pure water (18.25 MΩ cm) was used to prepare all the solutions, which was obtained from a Milli-Q Direct 16 water purification system (Millipore, Bedford, MA, USA).

Carboxyl-functionalized MWCNTs. The MWCNTs were heated at 300 °C for 75 min to remove amorphous carbon, graphite nanoparticles and catalyst impurities. Then, 0.50 g of treated MWCNTs was dispersed in 100 mL nitrifying mixture solution (H_2SO_4 : HNO_3 = 3 : 1 v/v). The mixture was sonicated for 45 min and then stirred under magnetic stirring at 75 °C for 12 h. After the reaction was completed, the solid was filtered through a 0.45 μm polycarbonate membrane and washed several times with ultrapure water until the pH was neutral. Finally, the filtered solid was dried at 70 °C overnight to obtain the carboxyl-functionalized MWCNTs (MWCNTs-COOH).

Synthesis of the magnetic MWCNTs/Fe_3O_4 nanocomposite (MMWCNTs–COOH). In total, 0.250 g MWCNTs–COOH, 0.745 g $FeSO_4 \cdot 7H_2O$ and 0.383 g $FeCl_3 \cdot 6H_2O$ with 100 mL water were added into a three-neck flask in a 70 °C bath. After that, 10 mL 0.5 M NaOH was added dropwise to the solution under nitrogen atmosphere and stirring. The mixture was performed at 70 °C for 24 h. Finally, the magnetic carbon nanotubes were prepared.

Preparation of MMWCNTs@Cs(I)-IIP and MMWCNTs@-NIP. The MMWCNTs@Cs(I)-IIP were prepared by surface imprinting polymerization. In total, 0.50 g MMWCNTs–COOH, 2.0 g chitosan and 0.40 g CsCl were dissolved in 150 mL 2% acetic acid aqueous. The mixture solution was sonicated for 45 min. Then, Span-80 as a surfactant, ammonium persulfate and sodium bisulfate as initiators, and glutaraldehyde solution as the cross-linking agent were added sequentially. Upon completion of the 12 h reaction under stirring of return flow and a nitrogen environment, the mixture was cooled to room temperature, and the magnetic composite material (unleached MMWCNTs@Cs(I)-IIP) was separated with a permanent magnet. Chelated Cs(I) was removed from the MMWCNTs@Cs(I)-IIP by rinsing with HCl (1.0 M) for 24 h. The eluates were analyzed by FAAS to ensure that there was no Cs(I) left in the polymer (Table S1†). The solid was dried at 60 °C for 24 h to obtain the leached MMWCNTs@Cs(I)-IIP. A non-imprinted magnetic multi-walled carbon nanotube polymer (MMWCNTs@-NIP) was prepared as a blank, without the addition of CsCl.

Preparation of the sensor MMWCNTs@Cs(I)-IIP/GCE. Glassy Carbon Electrodes (GCEs) were polished to a bright surface with an abrasive powder, and the electrodes were rinsed repeatedly with ultrapure water and dried at room temperature. In total, 20 mg PVC, 10 mg IIP, 20 mg NaTPB, 50 μL NPOE, 10 μL Nafion solution and 2.5 mL THF were thoroughly mixed, and the mixture was homogenized with an ultrasonic device until viscous. The mixture was poured into a glass dish, and the polished glassy carbon electrode was immersed in the mixture for 5–10 s. It was then taken out and allowed to dry at room temperature to form a thin PVC film on the surface of the GCE. By accurately weighing the weight of the electrode before and after deposition, the amount of the Cs-IIP material deposited on the GCE is about 0.2 mg. The prepared electrodes were conditioned for 48 h in a 1.0×10^{-4} M Cs solution at pH 6.5.

Analytical procedure

All the electrochemical measurements were obtained with a three-electrode system. MMWCNTs@Cs(I)-IIP/GCE were employed as the working electrode with a potassium chloride saturated calomel electrode (SCE) and a Pt sheet electrode as the reference and auxiliary electrodes, respectively.

The electrochemical cell employed for the potentiometric device add to the Fig. S1.† The response of the fabricated sensor was examined by measuring the potentials of the following electrochemical cell:

$$Hg, Hg_2Cl_2, KCl\ (satd)\|test\ solution|working\ electrode.$$

The PVC membrane electrode was scanned several times in a blank matrix electrolyte solution until a stable electrochemical signal was obtained. After each experiment, the membrane electrode was stirred in a 0.6 M HCl solution for 10 min to elute ions adsorbed on the surface of the membrane electrode. The potentials were measured by varying the concentration of Cs(I) in test solutions over a range of 1.0×10^{-8} to 1.0×10^{-1} M, and

the pH of test solutions was adjusted to 6.5. The calibration curve was determined by plotting the potential *E*, *versus* the logarithmic values of the Cs(I) concentration.

Results and discussion

The preparation and characterization of the MMWCNTs@Cs(I)-IIP

A feasible strategy for the preparation of the MMWCNTs@Cs(I)-IIP is shown in Scheme 1. The multi-walled carbon nanotubes were carboxylated with nitric acid and sulfuric acid system. The obtained carboxylated carbon nanotubes further interact with iron ions (Fe^{2+} : Fe^{3+} molar ratio = 2 : 1) to prepare magnetic multi-walled carbon nanotubes (MMWCNTs) in sodium hydroxide solution. Then the Cs(I) ion-imprinted polymer composite MMWCNTs@Cs(I)-IIP was synthesized by surface-imprinting technique, using MMWCNTs, Cs(I) ion, chitosan and glutaraldehyde as supporter, template ion, functional monomer and cross-linking agent respectively.[31–33] The –COOH groups coated on the magnetic MWCNTs' surface resulted in the imprinted layer structure being constructed. In this reaction, ammonium persulfate and sodium bisulfite together form a redox initiation system, which uses oxygen radicals generated by electron transfer between an oxidizing agent and a reducing agent to start a polymerization reaction. The advantage of this method is that the reaction rate can be increased, and the activation energy of the entire polymerization reaction can be reduced.[34,35]

FT-IR spectra were obtained to characterize the chemical structures of the raw-MWCNTs, MWCNTs–COOH, unleached MMWCNTs@Cs(I)-IIP and leached MMWCNTs@Cs(I)-IIP. The results are shown in Fig. 1. The spectra of the leached-IIP and unleached-IIP were basically consistent, indicating there was no significant effect on the backbone of the polymer after elution and removal of Cs(I). In the spectrum of the MWCNTs–COOH, the peak at 1402 cm^{-1} was attributed to C–O stretching, while the peak at 1639 cm^{-1} was attributed to the vibrations of the COOH band.[36] The characteristic peaks at 1950 and 969 cm^{-1} were attributed to the stretching vibrations of C=O and CH–CH_2. Noticeable N–H and O–H stretching vibration adsorptions can be seen at 3540 cm^{-1}, indicating that a polymer may be wrapped around the surface of the carbon nanotubes.

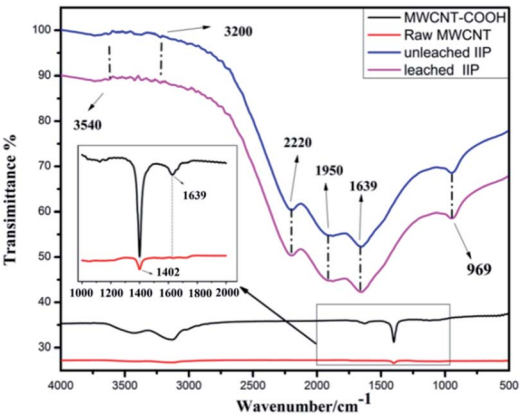

Fig. 1 The FT-IR spectra of the raw-MWCNTs, MWCNTs–COOH, unleached MWCNTs@Cs(I)-IIP and leached MWCNTs@Cs(I)-IIP.

The XRD patterns of the raw MWCNTs, MMWCNTs@Cs(I)-IIP are shown in Fig. 2. The diffraction peak at $2\theta = 26.02°$ corresponds to the (002) planes of the raw MWCNTs, which was observed for both the Fe_3O_4@MWCNTs and MWCNTs@Cs(I)-IIP. The diffraction peaks at $2\theta = 30.09°$, 35.46°, 43.24°, 53.40°, 57.13° and 62.54° correspond to the (220), (311), (400), (422), (511) and (440) planes.[37] It shows that Fe_3O_4 magnetic core was successfully introduced into MWCNTs. Since the imprinted layer materials are all amorphous structures, no other diffraction peaks can be observed in the XRD spectrum.

The surface morphologies of the raw MWCNTs and MWCNTs@Cs(I)-IIP were characterized with SEM and TEM. In Fig. 3a and c, the MWCNTs exhibit a threadlike nanotube structure with a diameter ranging from 8 to 10 nm. As shown in Fig. 3b and d, after functionalization of the MWCNTs followed by the polymerization process, the Fe_3O_4 nanoparticles and the imprinted polymer layer were grafted on the MWCNTs surface,

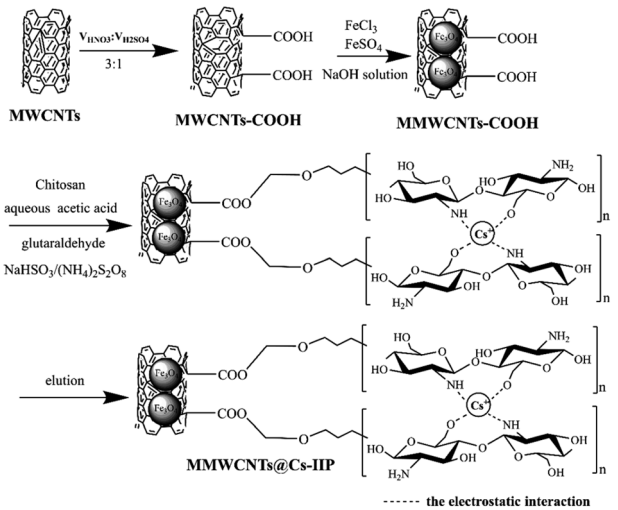

Scheme 1 The preparation process for MMWCNTs@Cs(I)-IIP.

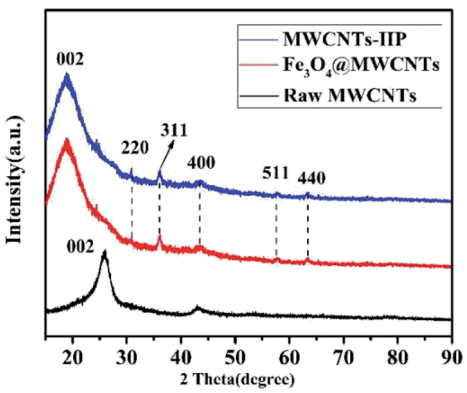

Fig. 2 The XRD patterns of the raw MWCNTs, Fe_3O_4@MWCNTs and MWCNTs@Cs(I)-IIP.

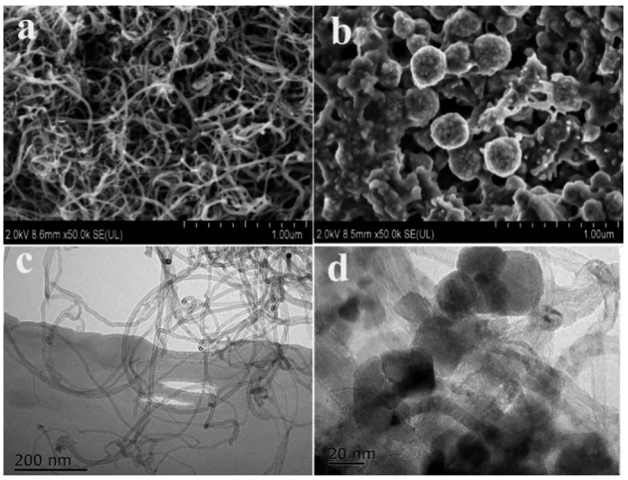

Fig. 3 SEM images of Raw MWCNTs (a), and MMWCNTs@Cs(I)-IIP (b), TEM images of raw MWCNTs (c) and MMWCNs@Cs(I)-IIP (d).

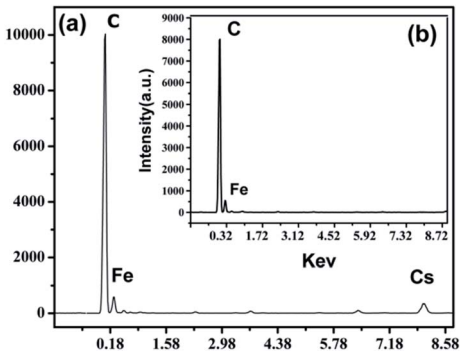

Fig. 4 EDS spectra of the unleached MMWCNTs@Cs(I)-IIP (a) and the leached MMWCNTs@Cs(I)-IIP (b).

and the diameter of the MWCNTs was obviously increased. The strong combination of Fe_3O_4 nanoparticles and MWCNTs can be attributed to covalent interactions through functional groups on the surface of the modified MWCNTs. The MMWCNTs@Cs(I)-IIP exhibited a coagulated structure and a rough surface, which may be due to agglomeration on the surface of the polymer. As a result, the rough surface structure favors mass transfer and the formation of three-dimensional recognition sites. The results demonstrate that the preparation process of the magnetic imprinted materials was successful.

EDS analysis is commonly performed to determine the elemental composition of materials. As shown in Fig. 4, C is the main element of the MWCNTs, and the appearance of a Fe signal indicates that the MWCNTs were successfully magnetized. The Cs signal was observed clearly in the unleached MMWCNTs@Cs(I)-IIP sample (Fig. 4a) and disappeared after extraction (Fig. 4b). These results indicate that the Cs(I) ion was successfully imprinted into the polymer, and Cs(I) can be easily extracted.

Electrochemical studies

The proposed ion-selective membrane consists of MMWCNTs@Cs(I)-IIP, additive (NaTPB), plasticizer (DBP or NPOE)[38] and PVC. In order to evaluate the effects of various components on the electrode efficiency, various kinds of GCEs coated membranes were fabricated, and their potentiometric responses in the presence of different concentrations of Cs(I) were examined. The results obtained are summarized in Table 1. The MWCNTs@Cs(I)-IIP is necessary for a considerable sensitivity and Nernstian response of the electrode. The plasticizers strongly influenced the working concentration range of the GCEs. The membranes prepared based on the NPOE plasticizer exhibited better potentiometric characteristics in the ways of linear range and Nernstian slope. Moreover, the addition of NaTPB improved the Nernstian behavior of the electrode, which may be due to the ionic additive NaTPB reducing the anionic interference and the electrical resistance of the membrane. According to the results, the optimum potentiometric response was obtained with GCE 8 (20% PVC, 50% NPOE, 10% MMWCNTs@Cs(I)-IIP and 20% NaTPB), and this was selected as the optimum composition for the modified electrode.

Effect of the solutions pH value

The effect of pH on the current response of the sensor was studied in the pH range of 4.0–8.5. As shown in Fig. 5, the current responses increased by increasing the pH from 4.0 to 6.5, and then decreased when the solution pH exceeded 6.5. The small current response at lower pH may be caused by the competitive adsorption of hydrogen ions, and the decrease of the current at high pH may be due to a decrease in the adsorption capacity of IIP under alkaline conditions.

Table 1 Compositions of the proposed sensor and their potentiometric response characteristics

	Composition (%)						
No.	PVC	Plasticizer	Cs-MIIP	NaTPB	Slope (V dec^{-1})	Linear range (mol L^{-1})	R^2
GCE1	20	NPOE (50)	—	20	0.02632	1×10^{-4} to 1×10^{-1}	0.98497
GCE 2	20	DBP (50)	—	20	0.01354	1×10^{-5} to 1×10^{-1}	0.94320
GCE 3	20	NPOE (50)	20	10	0.04667	1×10^{-4} to 1×10^{-1}	0.96916
GCE 4	20	DBP (50)	20	10	0.08469	1×10^{-6} to 1×10^{-1}	0.98987
GCE 5	10	DBP (50)	20	20	0.06618	1×10^{-7} to 1×10^{-4}	0.98772
GCE 6	10	NPOE (50)	20	20	0.04726	1×10^{-6} to 1×10^{-1}	0.97563
GCE 7	20	DBP (50)	10	20	0.03972	1×10^{-6} to 1×10^{-1}	0.99735
GCE 8	20	NPOE (50)	10	20	0.05904	1×10^{-7} to 1×10^{-4}	0.99725

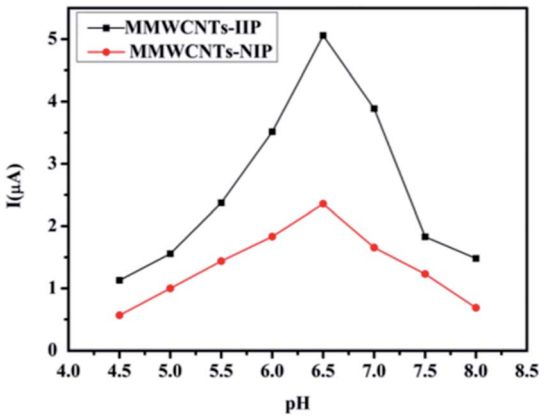

Fig. 5 Effect of pH on the current response of the optimized sensor toward 1.0×10^{-4} M Cs(I).

Response time, reproducibility and lifetime of the sensor

The response time is the average time required for the electrodes to reach the potential response within ± 1 mV of the final equilibrium value. The dynamic potential difference response of the sensor is shown in Fig. 6, and the sensor had a short response time of less than 5 s. To demonstrate the reproducibility of the sensor, potential measurements were performed on Cs(I) solutions with concentration ranges from 1×10^{-7} to 1×10^{-4} M. The obtained real-time-dependent potential measurements are shown in Fig. 7. The sensor response was highly reproducible, and the proposed sensor functioned for 6 weeks without significant potential deviation.

Analytical characteristics of the MMWCNTs@Cs(I)-IIP/GCE

A calibration curve of the MMWCNT@Cs(I)-IIP/GCE was constructed under the optimum conditions and is shown in Fig. 8. A linear relationship with a slope of 0.05954 V dec^{-1} was obtained between the response potential and the logarithm of the Cs(I) concentration over a range of 1×10^{-7} to 1×10^{-4} M. The linear regression equation is as follows: $E(V) = 0.05954 \log[Cs^+] - 0.4804$ ($R^2 = 0.999$). The limit of detection (DEC), as determined from the intersection of the two extrap olated segments of the calibration graph,[39] was 4.0×10^{-8} M. Due to the lack of specific Cs(I) recognition cavity in MNIP, MNIP/GCE does not have a good linear response and Nernst slope.

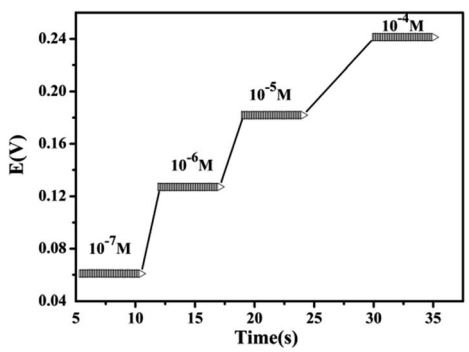

Fig. 6 Dynamic response of the MMWCNTs@Cs(I)-IIP/GCE with stepwise concentration changes of Cs(I).

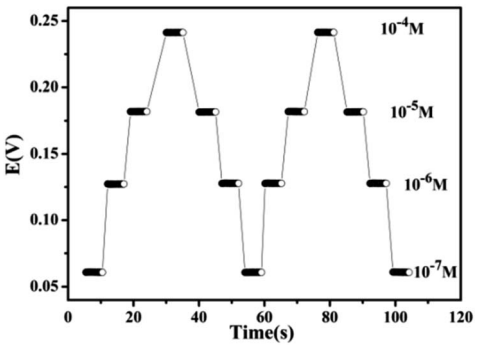

Fig. 7 Reproducibility of the MMWCNTs@Cs(I)-IIP/GCE.

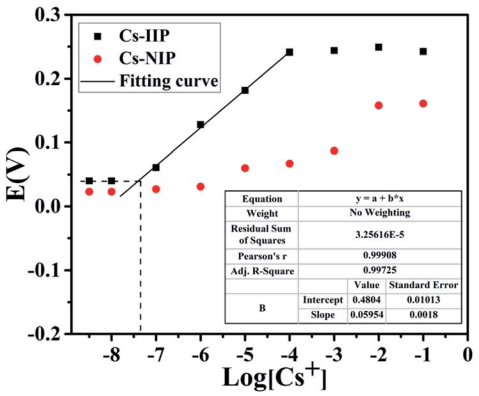

Fig. 8 Calibration curve of the developed MMWCNTs@Cs(I)-IIP/GCE and MMWCNTs@Cs(I)–NIP/GCE obtained at the optimized conditions.

Potentiometric selectivity

The selectivity coefficient (K) is the ability of a given ion-selective electrode to distinguish between interfering ions and the target ion. The potentiometric selectivity coefficients of the GCE 8 for different cationic species were determined by the matched potential method (MPM), which is independent of the Nikolsky–Eisenman equation.[40] The selectivity coefficient values were calculated by formula (1):

$$K^{\text{pot}}_{\text{Cs,M}} = \frac{a'_{\text{A}} - a_{\text{A}}}{a_{\text{B}}} \quad (1)$$

A specified activity (concentration) of the primary ion ($a'_{\text{A}} = 1.0 \times 10^{-5}$M for Cs(I)) was added to a reference solution (a_{A} of 1.0×10^{-6} M for Cs(I)), and the potential was measured.

Table 2 Potentiometric selectivity coefficients ($K^{\text{pot}}_{\text{CS,M}}$) of the sensor

M^{n+}	$K^{\text{pot}}_{\text{CS,M}}$ Cs-MIIP	Cs–NIP	M^{n+}	$K^{\text{pot}}_{\text{CS,M}}$ Cs-IIP	Cs–NIP
Li^+	1.0×10^{-2}	0.2	Mn^{2+}	5.0×10^{-3}	3.0×10^{-2}
Na^+	8.0×10^{-2}	0.16	Fe^{3+}	2.0×10^{-3}	1.4×10^{-2}
K^+	5.0×10^{-2}	0.13	Cu^{2+}	2.0×10^{-3}	6.3×10^{-2}
Rb^+	4.0×10^{-2}	0.25	Mg^{2+}	1.0×10^{-3}	8.3×10^{-2}

Table 3 Comparison of the proposed sensor with various reported electrodes

	Potentiometric behavior		$(-\log K^{pot}_{Cs,M})$			
Ionophore	Linear range	Detection limit (M)	K^+	Na^+	Application	Ref.
2,3-Benzoquino-crown	10^{-4} to 10^{-1}	2.5×10^{-5}	0.99	2.38	None	42
Calix[4]crown ether ester	5×10^{-6} to 10^{-1}	5.0×10^{-6}	2.00	1.30	None	43
5-(4-Nitrophenylazo)25,27-bis(2-propyloxy)[26,28]	10^{-5} to 10^{-1}	4.6×10^{-6}	2.27	3.13	None	44
Thiacalix[4]biscrown-6,6	10^{-6} to 3.6×10^{-2}	3.8×10^{-7}	3.70	4.30	None	45
P-isopropylcalix[6]arene	10^{-6} to 10^{-1}	1.0×10^{-6}	2.62	2.74	Ground waters	46
1,3-Cyclotetradecyloxy calix[4] arene crown ether	10^{-7} to 10^{-2}	3.7×10^{-8}	2.13	4.08	Nuclear waste water streams	47
Cs-MIIP (our previous publication)	10^{-6} to 10^{-1}	3.0×10^{-7}	1.92	1.37	Tap water and brine	30
MMWCNTs@Cs(I)-IIP	10^{-7} to 10^{-4}	4.0×10^{-8}	1.30	1.09	River; industrial waste water and brine	This work

Table 4 Determination of cesium in real samples and comparison with ICP-MS values

Sample	Spiked Cs^+/(mol L^{-1})	Found[a] Cs^+/(mol L^{-1})	RSD% ($n = 3$)	ICP-MS/(mol L^{-1})	RSD% ($n = 3$)	Recovery/(%)
Brine	—	Not detected	—	Not detected	—	—
	3.0×10^{-6}	3.34×10^{-6}	0.8	3.17×10^{-6}	0.1	105.36
	1.0×10^{-5}	1.09×10^{-5}	0.7	1.03×10^{-5}	0.3	105.82
Beichuan river water	—	Not detected	—	Not detected	—	—
	3.0×10^{-6}	2.88×10^{-6}	0.8	2.93×10^{-6}	0.1	98.29
	1.0×10^{-4}	9.12×10^{-5}	0.6	9.62×10^{-5}	0.5	94.80
Industrial waster water	—	Not detected	—	Not detected	—	—
	3.0×10^{-6}	3.69×10^{-6}	0.8	3.51×10^{-6}	0.6	105.13
	1.0×10^{-5}	9.85×10^{-6}	0.7	1.03×10^{-5}	0.3	95.63

[a] The average value of three determinations.

In a separate experiment, interfering ions (a_B) were successively added to an identical reference solution, until the measured potential matched that obtained with the addition of the primary ions. The selectivity coefficient is given by the ratio of the resulting primary ion activity to the interfering ion activity (concentration).[41] The selectivity coefficients $K^{pot}_{Cs,M}$ of the sensor for Cs(I) ions over other M^{n+} cations, obtained *via* the described method, are summarized in Table 2. The depicted results indicate that the sensor is noticeably selective to Cs(I) ions in the presence of most of the interfering ions tested. Therefore, the MMWCNTs@Cs(I)-IIP/GCE could be recommended for use in the determination of Cs(I) ions in samples with a complicated matrix.

Comparison of the present sensor with previously reported Cs(I) sensors

We compared the properties of our sensor with some previously reported Cs(I) selective electrodes, as shown in Table 3. Although the linear range of our sensor was not as wide as those reported, the as-prepared sensor had a lower DEC and high selectivity. The good electrochemical performance may be attributed to the Cs(I)-IIP and the specific surface area of the MWCNTs.

Real sample analysis

The utility of the sensor was also checked by applying the electrochemical method to measure the Cs(I) concentration in real water samples. The contents of Cs(I) and natural mineral impurities in the samples were detect by ICP-MS, and the results are listed in Table S2.† MMWCNTs@Cs(I)-IIP/GCE was used as selective electrode to carry out standard recovery experiments on these samples. Meanwhile, ICP-MS was chosen as a comparison technique. The results obtained are shown in Table 4. The results showed that the recoveries of Cs(I) ranged from 94.80% to 105.82% with RSDs less than 1.0%, and no significant differences between the Cs(I) concentrations obtained by the developed electrode and those given by the ICP-MS method were found. This demonstrates that the MMWCNTs@Cs(I)-IIP/GCE sensor is useful for direct determination of Cs(I) in real samples.

Conclusions

A simple, selective and sensitive ion-imprinted electrochemical sensor was developed for the rapid determination of Cs(I) in complex matrixes in the present work. The sensor was linearly dependent on cesium concentration over a range of 1×10^{-7} to 1×10^{-4} M with a detection limit of 4.0×10^{-8} M. The good sensitivity and lower limit of detection of the MMWCNTs@Cs(I)-IIP/GCE sensor toward cesium may be due to the synergistic effect caused by the IIP and MMWNCTs. The proposed imprinted sensor has been successfully applied for the detection of Cs(I) in complex real samples.

Author contributions

Zhiming Wang: investigation and writing. Long Wang: investigation and writing. Cuo Zhou: investigation. Chunyan Sun: supervision.

Conflicts of interest

There are no conflicts to declare.

Acknowledgements

This work was sponsored by the National Natural Science Foundation of China (No. 21766028), Qinghai Natural Science Foundation of China (No. 2018-ZJ-912).

Notes and references

1 M. P. Zheng and X. F. Liu, Hydrochemistry of Salt Lakes of the Qinghai-Tibet Plateau, *Aquat. Geochem.*, 2009, **15**, 293–320.

2 M. P. Zheng and X. A. Liu, Hydrochemistry and minerals assemblages of salt lakes in the Qinghai-Tibet Plateau, *Acta Geol. Sin.*, 2010, **84**, 1585–1600.

3 M. Arafat Mahmud, N. Kumar Elumalai, M. Baishakhi Upama, *et al.*, Cesium compounds as interface modifiers for stable and efficient perovskite solar cells, *.Sol. Energy Mater. Sol. Cells*, 2018, **174**, 172–186.

4 S. M. Liu, H. H. Liu and Y. J. Huang, Solvent extraction of rubidium and cesium from salt lake brine with t-BAMBP–kerosene solution, *Trans. Nonferrous Met. Soc. China*, 2015, **25**, 329–334.

5 F. Y. Wang, Solubility diagrams of Na_2SO_4–Rb_2SO_4–$MgSO_4$–H_2O, Na_2SO_4–Cs_2SO_4–$MgSO_4$–H_2O, and K_2SO_4–Cs_2SO_4–$MgSO_4$–H_2O at 298.15 K, *Russ. J. Inorg. Chem.*, 2017, **62**, 1111–1115.

6 N. Zhang, D. L. Gao and M. M. Liu, Effect of SO_2 Interval Fumigation on Color and Antioxidant Activity of Red Grape, *Adv. Mater.*, 2014, **1015**, 417–420.

7 J. H. Park, B. U. Chang, Y. J. Kim, J. S. Seo, S. W. Choi and J. Y. Yun, Determination of Low Cs (137) Concentration in Seawater Using Ammonium 12-molybdophosphate Adsorption And Chemical Separation Method, *J. Environ. Radioact.*, 2008, **99**, 1815–1818.

8 A. Dyer, A. Chimedtsogzol, L. Campbell and C. Williams, Uptake of caesium and strontium radioisotopes by natural zeolites from Mongolia, *Microporous Mesoporous Mater.*, 2006, **95**, 172–175.

9 S. J. Datta, W. K. Moon, D. Y. Choi, H. wang and I. C. Yoon, A Novel Vanadosilicate with Hexadeca-Coordinated Cs^+ Ions as a Highly Effective Cs^+ Remover, *Angew. Chem., Int. Ed.*, 2014, **35**, 28–38.

10 X. S. Yang, S. Y. Zhang and H. J. Li, Determination of Rubidium and Cesium in Chloride Type Oilfield Water by Flame Atomic Absorption Spectrometry, *Spectrosc. Spect. Anal.*, 2009, **29**, 833–839.

11 L. Cao, J. Zheng, H. Tsukada, S. Pan and Z. Wang, Simultaneous determination of radiocesium (135Cs, 137Cs) and plutonium (239Pu, 240Pu) isotopes in river suspended particles by ICP-MS/MS and SF-ICP-MS, *Talanta*, 2016, **159**, 55–63.

12 A. Zhang, J. Li, D. Ying and X. Lei, Development of a new simultaneous separation of cesium and strontium by extraction chromatograph utilization of a hybridized macroporous silica-based functional material, *Sep. Purif. Technol.*, 2014, **127**, 39–45.

13 H. Chen, F. Sun, J. Li, M. Dong and Z. Wei, Determination of trace ruthenium and cesium in rock salt by Icp-ms, *J. Spectroscopy Laboratory*, 2010, **27**, 1554–1556.

14 M. Shamsipur and H. R. Rajabi, Flame photometric determination of cesium ion after its preconcentration with nanoparticles imprinted with the cesium-dibenzo-24-crown-8 complex, *Microchim. Acta*, 2013, **180**, 243–252.

15 A. D. Savariraj, R. V. Mangalaraja, K. Prabakar, *et al.*, Electrochemical Aspects for Wastewater Treatment, *Green Methods for Wastewater Treatment*, 2019, pp. 121–179.

16 J. A. Squella, A. E. Iribarren, J. C. Sturm, *et al.*, Electrochemical Determination of Lacidipine, *J. AOAC Int.*, 2020, **5**, 1077–1082.

17 B. Li, Y. Wu, N. Li, *et al.*, Single Metal Atoms Supported on MBenes for Robust Electrochemical Hydrogen Evolution, *ACS Appl. Mater. Interfaces*, 2020, **12**, 9261–6267.

18 C. Branger, W. Meouche and A. Margaillan, Recent Advances on Ion Imprinted Polymers, *React. Funct. Polym.*, 2013, **73**, 859–875.

19 J. Fu, L. Chen, J. Li and Z. Zhang, Current status and challenges of ion imprinting, *J. Mater. Chem. A*, 2015, 1–43.

20 Z. L. Zhang, X. H. Xu and Y. S. Yan, Kinetic and thermodynamic analysis of selective adsorption of Cs(I) by a novel surface whisker-supported ion-imprinted polymer, *Desalination*, 2010, **263**, 97–106.

21 Z. Dahaghin, P. A. Kilmartin and H. Z. Mousavi, Determination of Cadmium(II) Using a Glassy Carbon Electrode Modified with a Cd-Ion Imprinted Polymer, *J. Electroanal. Chem.*, 2018, 810–816.

22 X. Cai, J. Li, Z. Zhang, F. Yang, R. Dong and L. Chen, Novel Pb^{2+} Ion Imprinted Polymers Based on Ionic Interaction *via* Synergy of Dual Functional Monomers for Selective Solid-Phase Extraction of Pb^{2+} in Water Samples, *ACS Appl. Mater. Interfaces*, 2014, **6**, 305–316.

23 T. Alizadeh and K. Atayi, Ion-Imprinted Polymer *via* Emulsion Polymerization and Its Use as the Recognition Element of Graphene/Graphite Paste Potentiometric Electrode, *Mater. Chem. Phys.*, 2018, **209**, 180–187.

24 F. Long, Z. Zhang, Z. Yang, J. Zeng and Y. Jiang, Imprinted Electrochemical Sensor Based on Magnetic Multi-Walled Carbon Nanotube for Sensitive Determination of Kanamycin, *J. Electroanal. Chem.*, 2015, **755**, 7–14.

25 T. Alizadeh and S. Nayeri, Mirzaee, A high performance potentiometric sensor for lactic acid determination based on molecularly imprinted polymer/MWCNTs/PVC nanocomposite film covered carbon rod electrode, *Talanta*, 2018, **15**, 103–111.

26 T. Alizadeh, S. Mirzaee and F. Rafiei, All-solid-state Cr(III)-selective potentiometric sensor based on Cr(III)-imprinted polymer nanomaterial/MWCNTs/carbon nanocomposite electrode, *Int. J. Environ. Anal. Chem.*, 2017, 1–15.

27 H. Negin and G. M. Reza, Alizadeh, Development of a highly selective and sensitive electrochemical sensor for Bi^{3+} determination based on nano-structured bismuth-imprinted polymer modified carbon/carbon nanotube paste electrode, *Sens. Actuators, B*, 2017, **245**, 605–614.

28 A. Archana and M. Beena, Electrochemical sensor based on nanostructured ion imprinted polymer for the sensing and extraction of Cr(III) ions from industrial wastewater, *Polym. Int.*, 2018, **67**, 1594–1604.

29 M. Roushani, Z. Saedi, F. Hamdi and B. Z. Dizajdizi, Preparation an electrochemical sensor for detection of manganese (II) ions using glassy carbon electrode modified with multi walled carbon nanotube-chitosan-ionic liquid nanocomposite decorated with ion imprinted polymer, *Electroanal. Chem.*, 2017, **804**, 1–6.

30 L. Wang, Z. M. Wang, C. Zhou, W. J. Song and C. Y. Sun, Potentiometric microsensor based on ion-imprinted polymer for the trace determination of cesium(I) ions, *J. Dispersion Sci. Technol.*, 2020, **41**, 1095–1103.

31 M. Rethinasabapathy, S. M. Kang, l. Lee, *et al.*, Highly stable Prussian blue nanoparticles containing graphene oxide–chitosan matrix for selective radioactive cesium removal, *Mater. Lett.*, 2019, **241**, 194–197.

32 H. Z. SHANG, J. N. HE, J. D. ZHAO, *et al.*, Preparation and Properties of Multi-walled Carbon Nanotubes and Chitosan Self-assembled Ion Imprinted Polymers, *Fine Chem.*, 2017, **11**, 1213–1225.

33 H. Q. Wang, H. Z. Shang, X. R. Sun, *et al.*, Preparation of thermo-sensitive surface ion-imprinted polymers based on multi-walled carbon nanotube composites for selective adsorption of lead(II) ion, *Colloids Surf., A*, 2020, **585**, 124139.

34 T. H. Bui, W. Lee, S. B. Jeon, K. W. Kim and Y. Lee, Enhanced Gold(III) adsorption using glutaraldehyde-crosslinked chitosan beads: Effect of crosslinking degree on adsorption selectivity, capacity, and mechanism, *Sep. Purif. Technol.*, 2020, **248**, 116989.

35 F. Zhao, X. P. Qin and S. Y. Feng, Microstructure, mechanical and swelling properties of microgel composite hydrogels with high microgel content and a microgel cluster crosslinker, *RSC Adv.*, 2015, **5**, 45113.

36 T. Majid and S. Hassanpour, Selective adsorption of Cr(VI) ions from aqueous solutions using a Cr(VI)-imprinted polymer supported by magnetic multiwall carbon nanotubes, *Polymer*, 2017, **132**, 1–11.

37 J. N. He, Synthesis and application of ion imprinting polymer coated magnetic multi-walled carbon nanotubes for selective adsorption of nickel ion, *Appl. Surf. Sci.*, 2018, **15**, 110–117.

38 M. M. Yusoff, N. R. N. Mostapa, M. S. Sarkar, T. K. Biswas, M. L. Rahman, S. E. Arshad, M. S. Sarjadi and K. A. D. ulkarni, Synthesis of Ion Imprinted Polymers for Selective Recognition and Separation of Rare Earth Metals, *J. Rare Earths*, 2017, **35**, 177–186.

39 M. R. Ganjali, M. R. Pourjavid, M. Rezapour and S. Haghgoo, Novel Samarium(III) Selective Membrane Sensor Based on Glipizid, *Sens. Actuators, B*, 2003, **89**, 21–26.

40 Y. Umezawa, K. Umezawa and H. Sato, Selectivity Coefficients for Ion-Selective Electrodes: Recommended Methods for Reporting ka, Bpot Values (Technical Report), *J. Pure Appl. Chem. Res.*, 1995, **67**, 507–518.

41 S. A. Rezvani Ivari, A. Darroudi and M. H. Arbab Zavar, Ion Imprinted Polymer Based Potentiometric Sensor for the Trace Determination of Cadmium(II) Ions, *J. Chem.*, 2017, **10**, S864–S869.

42 K. Kimura, A. Ishikawa, H. Tamura and T. Shono, Cheminform Abstract: Lipophilic Bis(Crown Ether) Derivatives of 15-Crown-5 and 18-Crown-6 as Neutral Carriers of Ion-Selective Electrodes, *Chem. Informationsdienst*, 1984, **15**, 447–450.

43 M. G. Fallon, D. Mulcahy, W. S. Murphy and J. D. Glennon, Caesium Ion-Selective Electrodes Based on Crowned Benzoquinones, *Analyst*, 1996, **212**, 127–131.

44 N. Simon, S. Eymard, B. Tournois and J. F. Dozol, Caesium extraction from acidic high level liquid wastes with functionalized Calixarenes, in: Proc. Int. Conf. on Scientific research on the back end of the fuel cycle for the 21st century, *J. Atlante.*, 2000, 24–26.

45 J. W. Ronny, R. Brzozka, Z. Casnati and A. Ungaro, Cesium-Selective Chemically Modified Field Effect Transistors with Calix[4]Arene-Crown-6 Derivatives, *Anal. Chim. Acta*, 1995, **301**, 263–267.

46 A. Radu, S. Peper, C. Gonczy, W. Runde and D. Diamond, Trace-Level Determination of Cs^+ Using Membrane-Based Ion-Selective Electrodes, *Electroanalysis*, 2006, **18**, 1379–1388.

47 P. S. Ramanjaneyulu, K. Kundu, M. K. Sharma and S. K. Nayak, Development of New Cs^+ Ion-Selective Electrode with Alkyl-Bridged Calix[4]Arene Crown-6 Compounds for the Determination of Cs^+ in Nuclear Waste Streams, *ChemistrySelect*, 2017, **2**, 10347–10353.